Intersection of non-matching grids of different dimensions

Jan Březina[a], Pavel Exner[a,*]

[a] *Technical University of Liberec, Studentská 1402/2, 461 17 Liberec 1, Czech Republic*

Abstract

TODO: An abstract.

Keywords: non-matching gird, intersections, mixed-dimensional mesh, Plückercoordinates

1. Introduction

Structure of introduction:
- motivation for computing mesh intersections, other applications - basic overview of existing work, approaches - our contribution - new algorithms for element intersectins based on Plücker coordinates - improvement of the front tracking algorithm

[1] - Use *g*eometric predicates incircle and orientation. Use mesh of bounding boxes to search for intersection candidates. Only use point queries for all vertices of triangle/tetrahedron. Use compatible partitioning of elements by the crack elements.

[2] - Implementation of the Nitche method in Fenics. They need 2d-3d intersections, but only for distribution od quadrature points. So they do not store whole intersection data, but only the quad points. The boundary of one domain is partitioned into intersections with elements of the other domain. Use
emph collision relations (pairs of faces of boundary and elmements of the background mesh) and *c*ollision maps (map face to all intersections and background element to all intersections, can be constructed from the collision relation), They cite books from computer graphics .. Mention geometric predicates. Present algorithms for: find intersection candidates, comput intersections, integrate over complex domains.

[3] Claim to provide robust algorithm covering all tiangle-trinagle degenerate cases. Basic idea is the same as our: use some tree (Binary SPace Tree) structure to find initial point on intersection curve and trace the curve in both

*Corresponding author.
Email addresses: jan.brezina@tul.cz (Jan Březina), pavel.exner@tul.cz (Pavel Exner)

directions. Quite clever data structure for the mesh. Adaptive precision geometric predicates. Store topological information about the intersection points (point on triangle, edge, vertex). Resolve various degenerate cases, dicuss mesh optimization after subdivision.

[4] Full algorithm for 2d=3D called PANG. Implemented in DUNE in 2010 (Bastian). Other software (Hecht, MpCCI). Triangle-Triangle and Tetra-Triangle intersections done similarly as in aur approach: set of points including vertices and then sort them countercolckwise. Local intersection algorithm do not provide neighbouring information so the traversal algorithm do not use it.

Review of algorithms: [5]

[6] Robust discretization of porous media. Complete error analysis with mortar non-compatible case. Seems they use normal fluxes accros fracture instead of pressure traces. This allows conforming discretization and error results.

[7] Application of mixed-dimensional approach in mechanics. Beam and shell elements ...

[8] Finite volume method, fully implicit two phase flow. Cite usage of FRAC3D generator.

[9] Space-time DG with adaptive mesh, need integration of product of functions on different meshes (in 2D). An algorithm for computing triangle-triangle intersections in 2D.

[10] DFN + MHFEM. Mortar method for intersections. Focused on formulation not on intersections.

[11] (Barbara) Mortad, non=matching, acustics. Theory, structured gird case. No complex intersections.

[12] Patent for curiosity.

[13] Immersed boundary. ??

[14] ??

[15]

[**?**] Original algorithm for line-thetrahedra intersections.

[**?**] Line-convex Polyhedra intersections using generalisation of line-clipping algorithm

1.1. Elements Intersections

The initial problem that occurs when working with incompatible meshes of combined dimensions is the efficient computation of intersections of the mesh subdomains, in particular 1D-2D, 1D-3D, 2D-3D. There is a piece of code in Flow123d at the moment which uses means of analytic geometry. In particular, it computes an intersection of a line and a plane in 3D by solving Gaussian elimination. However it is not effiecient and it does not provide barycentric coordinates explicitly. In this section, we present our latest work on this problematics.

The topic is studied in the bachelor and master thesis of Viktor Friš [**?**], who was supervised by Jan Březina. They suggested a solution, based on [**?**] for the two aspects of the problem:

itemsep=-3pt an efficient identification of the intersecting pairs of elements,

iitemsep=-3pt an efficient computation of the actual intersection for the single element pair.

The algorithm is based on the methods used in the computer graphics, in particular for the task (b) Plückercoordinates are employed to efficiently compute 1D-2D intersection in three-dimensional space.

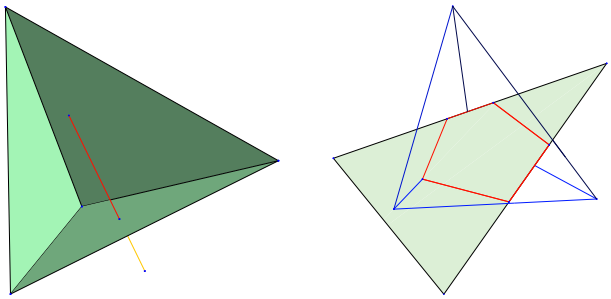

(a) 1D-3D (b) 2D-3D

For the 1D-3D and 2D-3D cases, the basic algorithm is applied on sides and edges of the simplices and all the topological information coming from the performed Plückerproducts is carefully collected to obtain final intersecting object. Further in 2D-3D case, an optimized tracing algorithm is suggested to directly obtain the correct order and orientation of the edges of the intersection polygon.

Viktor Friš provided an experimental implementation of the algorithm, on which we worked together in the end of his study. There is still a lot of work in the means of debugging, testing, and optimalization before it is applicable in Flow123d code. This task is being finalized at the moment by myself.

2. Intersection of elements

2.1. Plückercoordinates

Plückercoordinates represent a line in 3D space. Considering a line p, given by a point $\boldsymbol{A}$ and its directional vector $\boldsymbol{u}$, the Plückercoordinates of p are defined as

$$\pi_p = (\boldsymbol{u}_p, \boldsymbol{v}_p) = (\boldsymbol{u}_p, \boldsymbol{u}_p \times A).$$

Further we use a permuted inner product

$$\pi_p \odot \pi_q = \boldsymbol{u}_p \cdot \boldsymbol{v}_q + \boldsymbol{u}_q \cdot \boldsymbol{v}_p.$$

The sign of the inner product product gives us the relative position of the two lines, see Figure 1.

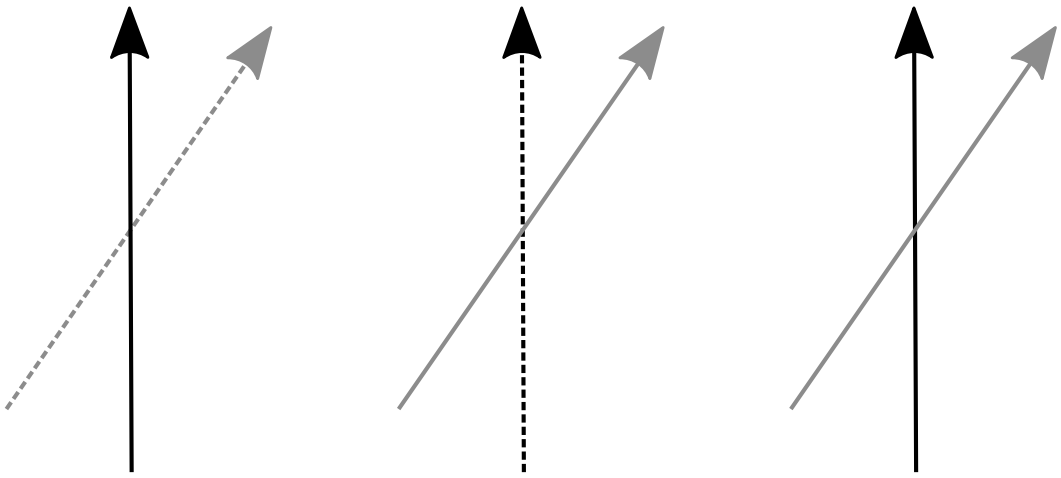

Figure 1: Sign of the Plückerproduct (from [**?**]). Dashed line symbolizes that the line is in the back. In the case (c), product is zero which means the lines intersect.

2.2. Intersection Line-Triangle (1D-2D)

Let us consider a line p and a triangle $(\boldsymbol{V}_0, \boldsymbol{V}_1, \boldsymbol{V}_2)$ with oriented sides $s_i = (V_j, V_k)$, $j = (i+1)mod3$, $k = (i+2)mod3$. The inner products $\pi_p \odot \pi_{s_i}$, $i = 0, 1, 2$ have the same sign if and only if there is an intersection point inside the triangle. In such a case, the inner products provides scaled barycentric coordinates of the intersection on the triangle. In particular for the baricentric coordinate w_i related to the vertex V_i we have

$$w_i = \frac{\pi_p \odot \pi_{s_i}}{\sum j = 0^2 \pi_p \odot \pi_{s_i}}$$

Indeed, using the barycentric coordinates the intersection point can be expressed as $\boldsymbol{X} = \boldsymbol{V}_0 + w_1\boldsymbol{s}_2 - w_2\boldsymbol{s}_1$. The line p have Plückercoordinates $(\boldsymbol{u}, \boldsymbol{u} \times \boldsymbol{X})$ (Plückercoordinates are invariant to change of initial point). Combining these two expressions we get

$$\pi_p \odot \pi_{s_1} = \boldsymbol{u} \cdot (\boldsymbol{s}_1 \times V_2) + \boldsymbol{s}_1 \cdot (\boldsymbol{u} \times [\boldsymbol{V}_0 + w_1\boldsymbol{s}_2 - w_2\boldsymbol{s}_1]) = -w_1\boldsymbol{u} \cdot (\boldsymbol{s}_1 \times \boldsymbol{s}_2).$$

Since $\boldsymbol{s}_0 + \boldsymbol{s}_1 + \boldsymbol{s}_2 = 0$ we have $\boldsymbol{s}_1 \times \boldsymbol{s}_2 = \boldsymbol{s}_2 \times s_0 = \boldsymbol{s}_0 \times \boldsymbol{s}_1$ and thus

$$\pi_p \odot \pi_{s_i} = -w_i\boldsymbol{u} \cdot (\boldsymbol{v}_1 \times \boldsymbol{v}_2).$$

Although a kind of proof can be found in [] we provide an alternative proof here. Let us denote $\boldsymbol{X}$ the intersection. The line p have parametric equation $\boldsymbol{Y} = \boldsymbol{X} + t\boldsymbol{u}$ and Plückercoordinates $(\boldsymbol{u}, \boldsymbol{X})$. Then the permuted inner product is:

$$\pi_p \odot \pi_{s_i} = \boldsymbol{u} \cdot (\boldsymbol{v}_i \times \boldsymbol{V}_i) + \boldsymbol{v}_i \cdot (\boldsymbol{u} \times \boldsymbol{X}) =$$

When one of the products is zero then there might be an intersection on the side or at the vertex of the triangle. We shall call the later case *pathologic*.

Starting with 1D-2D intersecting simplices, all the Plückercoordinates and products must be computed at first. In case that all Plückerproducts are nonzero and the intersection point exists, its barycentric coordinates can be obtained directly. Otherwise one of the pathologic cases occurs

itemsep=-3pt 1 zero product: line intersects triangle side,

itemsep=-3pt 2 zero products: line intersects triangle at its vertex,

itemsep=-3pt 3 zero products: line intersects triangle at its vertex and:

itemsep=-3pt intersects also the opposite side,
iitemsep=-3pt is parallel to the opposite side,
iiitemsep=-3pt intersects also another triangle vertex.

Anyway, in the pathologic case, the intersection of a line and triangle side is solved analyticaly which leads to a system of two equations with three unknowns. This is then solved using Crammer's rule.

So far, we considered the line and the triangle sides as bisectors. If the 1D-2D intersection is the final object, we check that the found intersection point lies on the abscissas. Otherwise all the computed data are used for further computation. Apart from the coordinates of the intersection points, we also save temporarily its topology information (vertex, side or edge index).

1D-3D (abscissa-tetrahedron). Tetrahedron has six edges, so six Plückercoordinates and products are computed at most. These data are passed to 1D-2D algorithm described above, which is then run for each pair line – tetrahedron side. There might be two intersection points maximally, which are finally checked that they belong o abscissas. If the line has its boundary point inside the tetrahedron, the intersection line must be cut and coordinates of intersection point are interpolated. Pathologic cases are again carefully processed so we obtain the most extensive topology information we can. See [**?**] for detailed description of all possible cases.

2D-3D (abscissa-tetrahedron). The intersection of a triangle and a tetrahedron is a polygon with 7 vertices at maximum. The vertices are found as intersection points of either triangle side and tetrahedron or tetrahedron edge and triangle. Therefore we use both algorithms above for 1D-3D and 1D-2D, respectively. Data are again efficiently passed to lower dimensional problems, so 9 Plückercoordinates and 18 Plückerproducts are computed.

The array of intersection points is generally not sorted. We use two so called *tracing* algorithms and we intend to orient the edges of the polygon in the same direction as the triangle is oriented. If one of the intersection point is pathologic,

a general convex hull method is applied using the Monotone chain[1] algorithm. The points are sorted using only their barycentric coordinates.

An optimized algorithm has been suggested for non-pathologic cases. At this moment all the collected topology data come into play. The algorithm takes advantage by using only the data already computed and also lowers the complexity to $O(N)$, compared with the Monotone chain complexity $O(N \log N)$ (N being number of intersection points).

2.3. Prolongation algorithm

Consider now a complex mesh of combined dimensions consisting of *components*, which are sets of connected elements of the same dimension (1D, 2D), in the space of 3D elements (tetrahedrons). Obtaining of all the 1D-3D and 2D-3D intersections is based on finding the first two elements intersecting each other. Then we can prolongate the intersection by investigating neighbouring elements of the component.

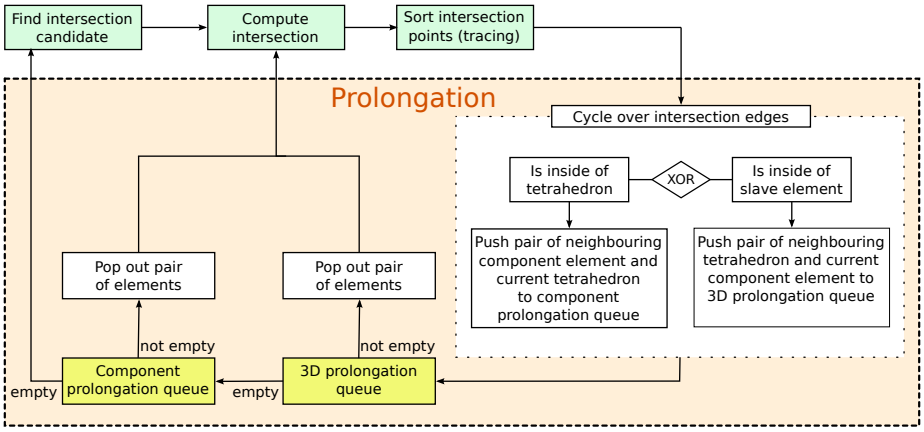

Figure 2: Prolongation algorithm for 1D-2D and 2D-3D intersections.

The prolongation algorithm is the same for both 1D and 2D components, see Figure 2. It can be seen as a *breadth-first search* [2] algorithm on the graph of 1D and 2D elements, respectively.

After computing the intersection of a pair of elements (line or triangle vs tetrahedron), we fill two queues with element pairs as candidates for further intersection. If the intersection edge (point of line in 1D, edge of polygon in 2D) is inside the tetrahedron, not on its surface, we get a neighbouring element of the component and push it back together with the current tetrahedron into *component prolongation queue*. If the intersection edge is inside the *slave* element

[1] Wikibooks, [online 2016-03-01], http://en.wikibooks.org/wiki/Algorithm_Implementation/Geometry/Convex_hull/Monotone_chain

[2] Wiki, [online 2016-03-01], https://en.wikipedia.org/wiki/Breadth-first_search

(line or triangle), i.e. is on the surface of tetrahedron, we get a neighbouring element of the tetrahedron and push it back together with the current slave element into *3D prolongation queue*.

Then we empty the prolongation queues – the 3D prolongation queue at first, then the component prolongation queue. When both queues are empty, all intersections of a component have been found and we continue to look for another component.

The algorithm is now unified for 1D and 2D in contrast to [**?**], where the component prolongation queue is emptied at first.

3. Front tracking algorithm

4. Benchmarks

5. Conclusions

TODO: - line intersection tracking for accelerate 2D-2D intersections - better handling of special cases in paarticular in relation to prolongations - better calculation reuse (pass with prolongations) - optimisation of element intersection - skip unnecessary calculations

6. Acknowledgement

The paper was supported in part by the Project OP VaVpI Centre for Nanomaterials, Advanced Technologies and Innovations CZ.1.05/2.1.00/01.0005.

[1] N. Sukumar, N. Mos, B. Moran, T. Belytschko, Extended finite element method for three-dimensional crack modelling 48 (11) 1549–1570. doi:10.1002/1097-0207(20000820)48:11<1549::AID-NME955>3.0.CO;2-A.
URL http://doi.wiley.com/10.1002/1097-0207%2820000820%2948%3A11%3C1549%3A%3AAID-NME955%3E3.0.CO%3B2-A

[2] A. Massing, M. G. Larson, A. Logg, Efficient implementation of finite element methods on nonmatching and overlapping meshes in three dimensions 35 (1) C23–C47. doi:10.1137/11085949X.
URL http://epubs.siam.org/doi/abs/10.1137/11085949X

[3] A. H. Elsheikh, M. Elsheikh, A reliable triangular mesh intersection algorithm and its application in geological modelling 30 (1) 143–157. doi:10.1007/s00366-012-0297-3.
URL http://link.springer.com/article/10.1007/s00366-012-0297-3

[4] M. J. Gander, C. Japhet, Algorithm 932: PANG: Software for nonmatching grid projections in 2d and 3d with linear complexity 40 (1) 1–25. doi:10.1145/2513109.2513115.
URL http://dl.acm.org/citation.cfm?doid=2513109.2513115

[5] M. J. Gander, C. Japhet, An algorithm for non-matching grid projections with linear complexity, in: M. Bercovier, M. J. Gander, R. Kornhuber, O. Widlund (Eds.), Domain Decomposition Methods in Science and Engineering XVIII, no. 70 in Lecture Notes in Computational Science and Engineering, Springer Berlin Heidelberg, pp. 185–192, DOI: 10.1007/978-3-642-02677-5_19.
URL http://link.springer.com/chapter/10.1007/978-3-642-02677-5_19

[6] W. M. Boon, J. M. Nordbotten, Robust discretization of flow in fractured porous media.
URL http://arxiv.org/abs/1601.06977

[7] S. Bournival, J.-C. Cuillire, V. Franois, A mesh-geometry based approach for mixed-dimensional analysis, in: Proceedings of the 17th International Meshing Roundtable, Springer, pp. 299–313.
URL http://link.springer.com/chapter/10.1007/978-3-540-87921-3_18

[8] V. Reichenberger, H. Jakobs, P. Bastian, R. Helmig, A mixed-dimensional finite volume method for two-phase flow in fractured porous media 29 (7) 1020–1036.
URL http://www.sciencedirect.com/science/article/pii/S0309170805002150

[9] K. Sldkov, V. Dolej, Bakalsk prce: Integration of piecewise polynomial functions on non-matching grids.

[10] G. Pichot, J. Erhel, J.-R. de Dreuzy, A generalized mixed hybrid mortar method for solving flow in stochastic discrete fracture networks 34 (1) B86–B105.
URL http://epubs.siam.org/doi/abs/10.1137/100804383

[11] B. Flemisch, M. Kaltenbacher, S. Triebenbacher, B. Wohlmuth, Non-matching grids for a flexible discretization in computational acoustics 11 (2) 472–488. doi:10.4208/cicp.141209.280810s.
URL http://www.journals.cambridge.org/abstract_S1815240600002292

[12] Hybrid local nonmatching method for multiphase flow simulations in heterogeneous fractured media, u.S. Classification 703/2, 703/10; International Classification G06F17/50; Cooperative Classification G01V2210/646, E21B43/26, G01V1/30, E21B41/00, G01V1/301, G06F17/5018.
URL http://www.google.com/patents/US20140046636

[13] R. Mittal, G. Iaccarino, IMMERSED BOUNDARY METHODS 37 (1) 239–261. doi:10.1146/annurev.fluid.37.061903.175743.
URL http://www.annualreviews.org/doi/abs/10.1146/annurev.fluid.37.061903.175743

[14] S. J. Owen, A survey of unstructured mesh generation technology., in: IMR, pp. 239–267.
URL http://ima.udg.edu/~sellares/ComGeo/OwenSurv.pdf

[15] Y. A. Kuznetsov, Overlapping domain decomposition with non-matching grids 6 299–308.
URL http://emis.ams.org/proceedings/DDM/DD9/Kuznetsov.ps.gz